PHOTOCATALYTIC PROPERTIES OF NANO SIZED Ag_2ZrO_3 CATALYSTS SYNTHESIZED VIA A CO-PRECIPITATION PROCESS

[a]*G.S. Gaikwad, [b] S. R. Thakare, [c] N.T. Khati, [d] A. V. Wankhade, [a]S.K. Patle, [a]K. Gour

[a]* Department of Chemistry, J. L. Chaturvedi College of Engineering, Nagpur, M S.

[b] Department of Chemistry, Shri Shivaji Science College, Nagpur, M S.

[c] Department of Applied Chemistry, Priyadarshini College of Engineering, Nagpur, M S.

[d] Department of Chemistry, Visvesvaraya National Institute of Techanology (VNIT), Nagpur, M S.

Abstract

Photocatalytic degradation of organic pollutants by metal oxide has attracted significant attention by researchers because of its usefulness in handling environmental contaminants. Due to the fact that the photo-generated holes in the valence band and the photo-generated electrons in the conduction band of an excited semiconductor could serve as the oxidation and the reduction species respectively, photocatalysts having strong oxidation–reduction power are widely studied for environmental cleaning and for hydrogen generation from water splitting. TiO_2 based photocatalyst are often studied for degradation of dyes . Titanium dioxide is one of the most widely studied semi-conducting photocatalysts for the degradation of organic contaminants from water and air, because of its physical and chemical stability, high catalytic activity, high oxidative power, low cost and ease of production . However, though it is a good catalyst, its wide band gap (3.2 eV) limits TiO_2 use in UV region. Since only about 4% of the solar spectra falls in the UV range, it is appealing to develop efficient visible light-sensitive photocatalysts in view of the better utilization of solar energy.

Highly photocatalytically active nano silver Zirconate has been prepared by Co-precipitation method and the effect of silver modification was studied. The structural and optical properties were characterized by X-ray diffraction, Fourier transform IR, SEM, TEM and UV- VIS diffuse reflectance spectroscopy. The sharp peaks in the XRD patterns indicate a well crystalline of the prepared samples. The average particle size was determined from XRD powder pattern according to Debey–Scherrer's equation ($D_{XRD} = k \cdot \lambda / \beta \cdot \cos \theta$)where D_{XRD} is the average particle size, k is a constant , λ is the X-ray wave-length equal to 0.15406 nm and β is the half-peak width. The average particle size was 40-50 nm. The particle size and morphology of samples were examined by SEM technique shows agglomerate and spongy nature . TEM micrographs of sample shows

Ag_2ZrO_3 powder calcined at 400 ^{0}C was uniform, with a well-distributed spherical particle with a size about 50 nm.

The photocatalytic activity of these materials were studied by analyzing the degradation of an organic dye, methylene blue (MB) and it is found that silver zirconate calcined at 400 °C shows higher rate of degradation than that of commercial TiO_2 photocatalyst Degussa P-25. We attribute these observations to the extent of valence band hole production and the role of silver in trapping the conduction band (CB) electrons . The sensitizing property of the dye and electron scavenging ability of silver together constitute to the interfacial charge transfer process in such a way to utilize the photoexcited electrons.

Keywords: Silver zirconate, Photocatalysis, photocatalytic activity, Calcination, Methylene blue.

1. Introduction

Photocatalytic degradation of organic pollutants by metal oxide has attracted significant attention by researchers because of its usefulness in handling environmental contaminants [1,2]. Due to the fact that the photo-generated holes in the valence band and the photo-generated electrons in the conduction band of an excited semiconductor could serve as the oxidation and the reduction species respectively, photocatalysts having strong oxidation–reduction power are widely studied for environmental cleaning [3,4] and for hydrogen generation from water splitting [5,6]. TiO_2 based photocatalyst are often studied for degradation of dyes [7-10]. Titanium dioxide is one of the most widely studied semi-conducting photocatalysts for the degradation of organic contaminants from water and air, because of its physical and chemical stability, high catalytic activity, high oxidative power, low cost and ease of production . However, though it is a good catalyst, its wide band gap (3.2 eV) limits TiO_2 use in UV region. Since only about 4% of the solar spectra falls in the UV range, it is appealing to develop efficient visible light-sensitive photocatalysts in view of the better utilization of solar energy. In attempts to prepare visible light-sensitive photocatalysts, some cation ion- or anion ion-doped TiO_2 [11-13] and some multiple-metal oxides [14,15] have been fabricated for organic compounds degradation

or water splitting. Among a variety of multiple-metal oxide photocatalysts, special attention was paid to materials containing metal ions with specific nd^{10}, ns^2 outer layer-orbital configurations, such $CaIn_2O_4$ [16], $AgInW_2O_8$ [17], $AgNbO_3$ [18], and $AgGaO_2$ [19]. As a common feature, the completely filled nd^{10} or (nd^{10}) ns^2 outer layer orbitals can hybridize with the O $2p^6$ orbitals in the valence band of a semiconducting material, pushing up the valence band top, and thus leading to a narrowed band gap. The modification of semiconductors with noble metals like platinum (Pt), silver (Ag), gold (Au) has attracted significant attention especially in heterogeneous Photocatalysis [20, 21]. Ag doped $NiTiO_3$, $AgSbO_3$, Ag_2ZnGeO_4 are used for degradation of dyes under visible light irradiation [22-24].

Zirconium dioxide is an important material widely used in ceramics technology [25] and heterogeneous catalysis with band gap energy of 5.0 eV [26] (reported values range between 3.25 and 5.1 eV [6] depending on the preparation technique of the sample but the most frequent and accepted value is 5.0 eV). Due to its nature as n-type semiconductor it has been considered recently as a photocatalysts in photochemical heterogeneous reactions [27-29].

In this work we analyze the effect of modifying ZrO_2 Semiconductor with silver a noble transition series cation trying to correlate the modification of the electronic properties with the catalytic activity (Fig. 1).

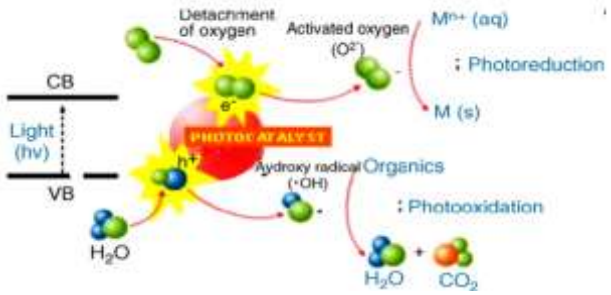

Fig.1. Scheme of the photocatalytic process.

2. Experimental Section

2.1 Sample Preparation

A visible-light-active photocatalyst nano Ag_2ZrO_3 was prepared by a simple co-precipitation method. High-purity $AgNO_3$ (99.9% Merck) and $ZrOCl_2$.$6H_2O$ (99.9% Merck) were use as raw materials. The solution 0.1 M $AgNO_3$ and 0.1 M $ZrOCl_2$.$6H_2O$ were mixed in 2:1 ratios. The pH value of the above solution was adjusted to 10.0 by a drop wise addition of concentrated ammonia solution. The resulting white precipitate was washed with distilled water for several times, and then dried, smashed and calcined at 700-800 ◦C. Thus, the target photocatalyst nano Ag_2ZrO_3 was obtained.

2.2 Characterization of sample

The crystal structure and phase purity were determined with X-ray diffractometer (XPERT-PRO Diffractometer) with monochromatic Cu α K radiation (45 kV, 40 mA). Microstructural characterization was performed by scanning electron microscopy (SEM) using a Jeol apparatus (model JSM-5400) and transmission electron microscopy (TEM) using a Philips CM200 instrument. The diffuse reflectance spectra (DRS) of the photocatalyst were measured by UV-visible spectrophotometer (UV-1800, Shimadzu) over spectral range 200 – 800 nm. The concentrations of aqueous methylene blue were determined by measuring the absorbance with an UV-visible spectrophotometer.

2.3 Photocatalytic Activity Mesurment

The photocatalytic activity of the prepared nano Ag_2ZrO_3 - CP Powder calcined at 400 ^{0}C for 24 hrs. was evaluated using methylene blue as a model organic compound. Doubly distilled water was used for the preparation of all solutions required for the experiment. The photocatalytic experiments were conducted in a a circular glass reactor (designed and fabricated in our laboratory) under the illumination of Halogen lamp (40W/230V/36D, Phillips) which predominantly emits at 425 nm with a definite power of 40W. For each condition, the reaction

suspension was prepared by adding 0.1g catalysts into a 100 ml methylene blue solution with an initial concentration of 1 x 10^{-5}M. The suspension was subjected to ultrasonic dispersion for 15min, and then magnetically stirred for 30 min in the dark to ensure the equilibrium of absorption/desorption between dye molecules and photocatalysts. Then the suspension was irradiated by the halogen lamp. During the photodegradation process, the halogen lamp was positioned horizontally above the surface of the suspension. The distance between halogen lamp and the surface was set at 10 cm. Analytical samples (3ml) were taken out for measurement of absorption after interval of every 15 min and centrifugated to remove the particles. The degradation efficiency of photocatalysts was analyzed by UV–visible spectrophotometer (UV-1800, Shimadzu) at its maximum absorption wavelength of 465 nm. The MB degradation efficiency as a function of reaction time was calculated by the following equation:

% degradation of MB (η) = $(C_0 - C_t/C_0) \times 100 = (A_0 - A_t/A_0) \times 100$

where C_0 and A_0 are the initial concentration and absorbance of MB solution at 465 nm

3. Result And Discussion

Characterization of the prepared nano Silver Zirconate

X-ray diffraction (XRD) is used to identify the structure of the prepared Powder. Fig.1 shows XRD pattern of nano Ag_2ZrO_3 calcined at 400 ^{0}C for 24 hrs. The sharp peaks in the XRD patterns indicate a well crystalline of the prepared samples. The average particle size was determined from XRD powder pattern according to Debey–Scherrer's equation[30]

$(D_{XRD} = k \cdot \lambda / \beta \cdot \cos \theta)$

where D_{XRD} is the average particle size, k is a constant , λ is the X-ray wave-length equal to 0.15406 nm and β is the half-peak width. The average particle size was 40-50 nm.

The particle size and morphology of samples were examined by SEM technique (Scanning Electron Microscopy). Fig. 2. illustrate that nano Ag_2ZrO_3 powders heat treated at 400 ◦C shows agglomerate and spongy nature .

TEM micrographs of sample are shown in Fig.3. The nano Ag_2ZrO_3 powder calcined at 400 ^{0}C was uniform, with a well-distributed spherical particle with a size about 50 nm. The average particle size increased with increasing calcining temperature, suggesting a gradual growth of the nano-particles during the heating process. The average particle size was about 40 and 50 nm.

Information about the absorptive properties of Silver Zirconate can be obtained from diffuse reflectance UV–Visible spectroscopy. This is very important information for photocatalytic application as catalyst since it gives information about the band gap of semiconductors. The UV-visible diffuse reflectance Spectrum of the Ag_2ZrO_3 semiconductor annealed at 800^{0}C is shown in Figure 4. The dark brown colored Ag_2ZrO_3 sample exhibits broad and strong absorption in the range from 200 to 600 nm. The energy band gaps of samples could be calculated according to the equation that had been widely adopted for crystalline semiconductors [19]

$$\alpha h\nu = A (h\nu - Eg)^{n/2}$$

Here α, ν, A, Eg, and n are the absorption coefficient, incident light frequency, constant, band gap, and an integer (normally equal to 1, 2, 4, or 6), respectively.

4. Photocatalytic Activity of Prepared Material:

Photocatalytic activities of the resulting samples were investigated by the degradation of methylene blue (MB) in aqueous solution. Blue colour of the solution gradually diminished upon the visible light irradiation in the presence of photocatalysts, illustrating the degradation of MB. Total concentrations of all MB species were simply determined by the maximum absorption measurement. **Fig. 5, & Fig. 6** shows the decrease

of the concentration of MB versus irradiation time in the presence of the as-prepared silver Zirconate and self-degradation under visible light irradiation. It was found that the self-degradation of MB under visible light irradiation was not obvious, indicating the stabilization of MB under visible light irradiation.

5. Possible Visible Light Induced Degradation Mechanism:

The photocatalytic oxidation of organic compounds is mainly involves following processes: i) The photoabsorption of the semiconductor catalyst and generation of electron and hole ii) The transfer of charge carriers and the utilization of the charge carriers by the reactants. Ag_2ZrO_3 exhibited the ability to absorb visible light, which is attributed to the transition of the electrons from the VB (hybrid orbitals of O 2p and Ag 4d) to the CB (Zr 4d orbital) in the catalyst. Furthermore, the hybridization of the Ag 4d and O 2p levels makes the VB largely dispersed which favors the mobility of photoholes in the VB and is beneficial to the oxidation reaction. Thus, it has been found that silver is one of the elements that is able to make a valence-band position higher than O 2p orbitals. Therefore, it is reasonable to believe silver zirconate is an visible light active photocatalyst and MB could be degraded within a certain wavelength range of visible light over .

6. Conclusion

We here synthesized nano Ag_2ZrO_3 by Co-precipitation. This method is convenient and easy to handle. As prepared, Ag_2ZrO_3 was found to be active under visible light irradiation for degradation of dye methylene blue. It indicates stability of Ag_2ZrO_3. The present study indicates that, it was feasible to prepare visible light active Silver Zirconate with Co-precipitation Method.

References

A. Fujishima, T.N. Rao, and D.A. Tryk, (2000). J. Photochem. Photobiol. C 1, 1.

Z. Zou, J. Ye, K. Sayama, and H. Arakawa, (2001). Nature 414 : 625–627.

E. Gkika, A. Troupis, and A. Hiskia, (2006). E. Papaconstantinou, Appl. Catal. B 62, 28–34.

H. Fu, L. Zhang, W. Yao, and Y. Zhu, (2006). Appl. Catal. B 66, 100–110.

J. Tang, Z. Zou, and J. Ye, *(* 2003). J. Phys. Chem. *B, 107*,14265-14269.

W. Yao, and J. Ye, (2005). J. Phys. Chem. B 110, 11188–11195.

A. Syoufian, O.H. Satriya, and K. Nakashima, (2007). Catal. Commun. 8 (5) 755–759.

W.D. Wang, C.G. Silva, and J.L. Faria, (2007). Appl. Catal. B 70 (1–4) 470– 478.

I.M. Arabatzis,a T. Stergiopoulos,a D. Andreeva,b S. Kitova,c S.G. Neophytides, d and P. Falaras , (2003). Journal of Catalysis 220 : 127–135

I. Poulios, and I. Tsachpinis, (1999). J. Chem. Technol. Biotechnol. 74 : 349– 357.

D. Li, H. Haneda, S. Hishita, and N. Ohashi, (2005). Mater. Sci. Eng. B 117: 67– 75.

Q.W. Zhang, J. Wang, S. Yin, T. Sato, and F. Saito, (2004). J. Am. Chem. Soc. 87: 1161–1163.

J. Wang, S. Uma, and K.J. Klabunde, (2004). Appl. Catal. B 48 : 151–154.

H. Fu, C. Pan, W. Yao, and Y. Zhu, (2005). J. Phys. Chem. B 109 : 22432– 22439.

X.P. Lin, F.Q. Huang,W.D.Wang, K.L. Zhang, (2006). Appl. Catal. A. 307: 257–262.

J. Tang, Z. Zou, M. Katagiri, and T. Kako, (2004). J. Ye, Catal. Today 93–95 : 885–889.

J. Tang, Z. Zou, and J. Ye, (2003). J. Phys. Chem. B 107 14265–14269.

H. Kato, H. Kobayashi, and A. Kudo, (2002). J. Phys. Chem. B 106 :12441– 12447.

Y. Maruyama, H. Irie, and K. Hashimoto, (2006). J. Phys. Chem. B 110 : 23274– 23278.

Hermann, J. M., Tahiri, H., Ait-Ichou, Y., Lossaletta, G., Gonzalez- Elipe, and A. R., Fernandez, *(*1997). A. Appl. Catal., *B 13:* 219.

Kamat, P.V. (2002). J. Phys. Chem. B 106 : 7729.

Yi-Jing Lina, Yen-Hwei Changa, Guo-Ju Chenb, Yee-Shin Changc, and Yee- Cheng Chang, (2009). Journal of Alloys and Compounds 479 : 785–790.

Tetsuya Kako, Naoki Kikugawa, and Jinhua Ye, (2008). Catal. Today 131 : 197– 202.

Xiukai Li , Shuxin Ouyang , Naoki Kikugawa and Jinhua Ye, (2008). Appl. Catal. A: General 334, 51–58.

H.H. Kung, (1989). Transition Metal Oxides. Surface Chemistry and Catalysis Studies in Surface Science and Catalysis, Vol. 45, Elsevier, Amsterdam.

A. Corma, Chem. Rev. 95 (1995) 559. Y.M. Wang, S.W. Liu, M.K. Lu, S.F. Wang, F. Gu, X.Z. Gai, X.P. Cui, J.Pan, J. Mol. Catal. A: Chem. 215 (2004) 137.

G. Colón, M.C. Hidalgo, and J.A. Nav´ıo, (2002). Appl. Catal. A: General 231: 185–199.

J. Luka, M. Klementova , P. Bezdic˘ka , S. Bakardjieva , J. S ubrt, L. Szatma´ry, Z. Bastl, and J. Jirkovsky´ , (2007). Appl. Catal.B: Environmental 74 : 83–91.

S.G. Botta, J.A. Navio, M.C. Hidalgo, G.M. Restrepo, M.I. Litter, (1999). J. Photochem. Photobiol. A 129 (89).

Yamashita H, Ichihashi Y, Zhang SG, Matsumura Y, Souma Y, Tatsumi T, Anpo M , (1997). Appl Surf Sci 121: 305.

Figure Caption:

Figure1. X-ray diffraction patterns of prepared nano Ag_2ZrO_3 (CP) powder.

Figure2. SEM images for nano Ag_2ZrO_3 (CP) powder calcined at 400 ◦C.

Figure 3 : TEM images for nano Ag_2ZrO_3 (CP) powder calcined at 400 ◦C.

Figure 4: Diffuse Reflectance spectra (DRS) of the prepared nano Ag_2ZrO_3 (CP) Powder.

Figure 5: The changes in absorbance of MB solution by nano Ag_2ZrO_3.The Conc. of the catalyst was 1 g/l.

Figure 6**:** a) Photodegradation of 1 x 10^{-5} M MB at 662 nm by nano Ag_2ZrO_3 at Suspensions of catalyst 1 g/l as function of visible light irradiation time. b) self- degradation of MB under visible light rradiation

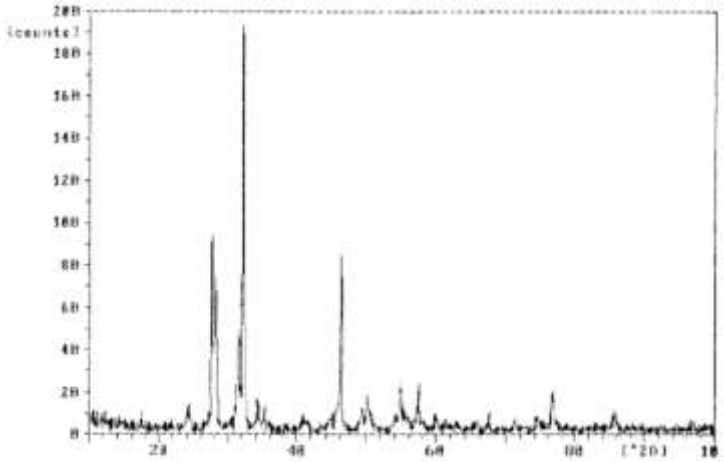

Figure1. X-ray diffraction patterns of prepared a) Ag_2ZrO_3 SSR b) Ag_2ZrO_3 powder after calcination at 400 ◦C .

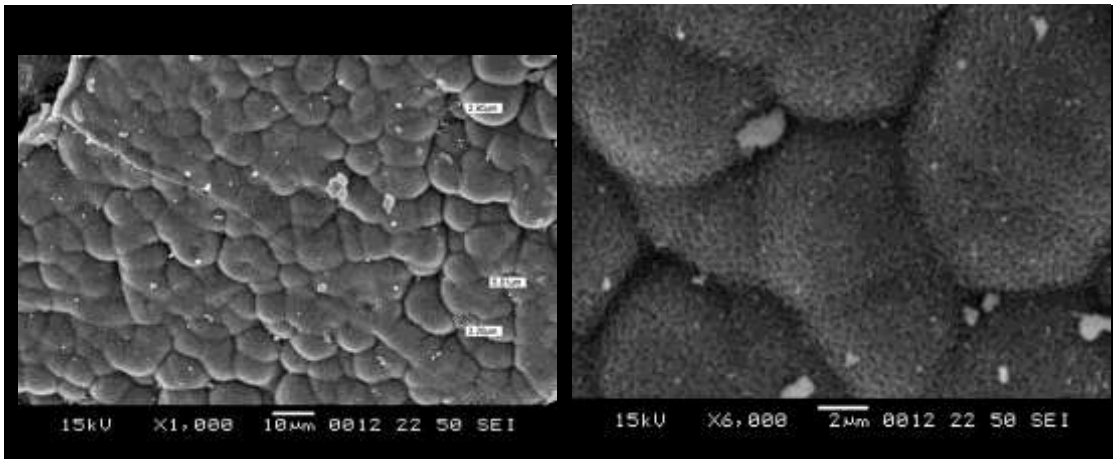

Figure 2. SEM images for Ag_2ZrO_3 (CP) powder calcined at 400 ◦C.

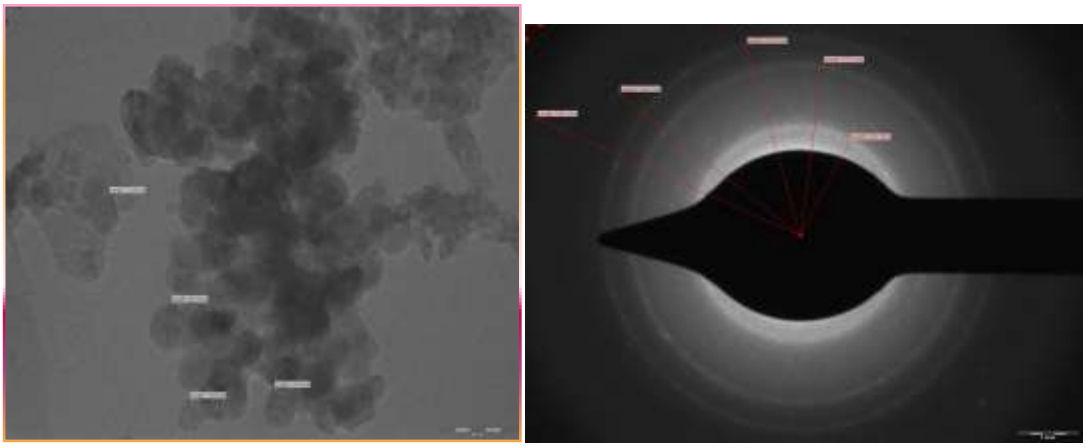

Figure 3. TEM images for Ag_2ZrO_3 (CP) powder calcined at 400 ◦C.

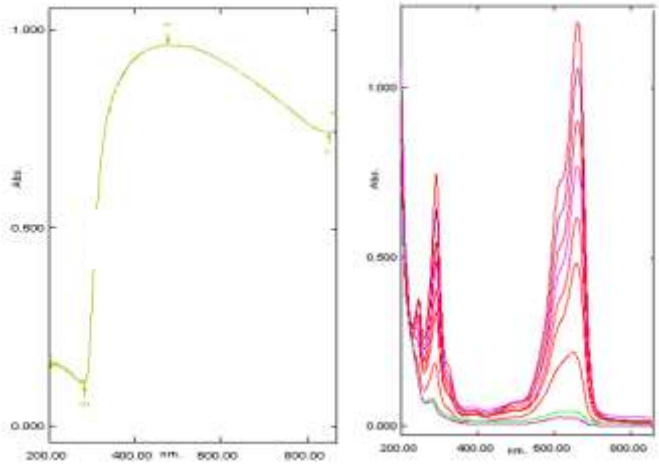

Figure 4: Diffuse Reflectance spectra (DRS) of the prepared Ag_2ZrO_3 (CP) powder calcined at 400^0C

Figure 5: The changes in absorbance of MB solution (1 x 10^{-5} M) by Ag_2ZrO_3 (CP).The conc. of the catalyst was 1 g/l.

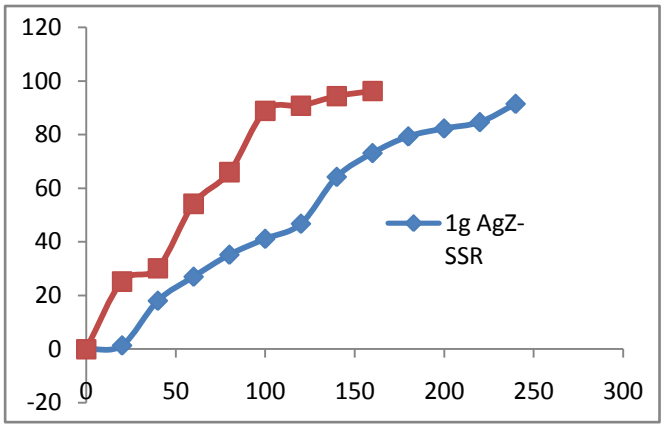

Figure 6:% Photodegradation of MB at 662 nm by Ag_2ZrO_3 SSR & AgZ-CP at initial conc.

1 x 10 $^{-5}$ M; the suspensions containing 1g/l as function of visible light irradiation time.